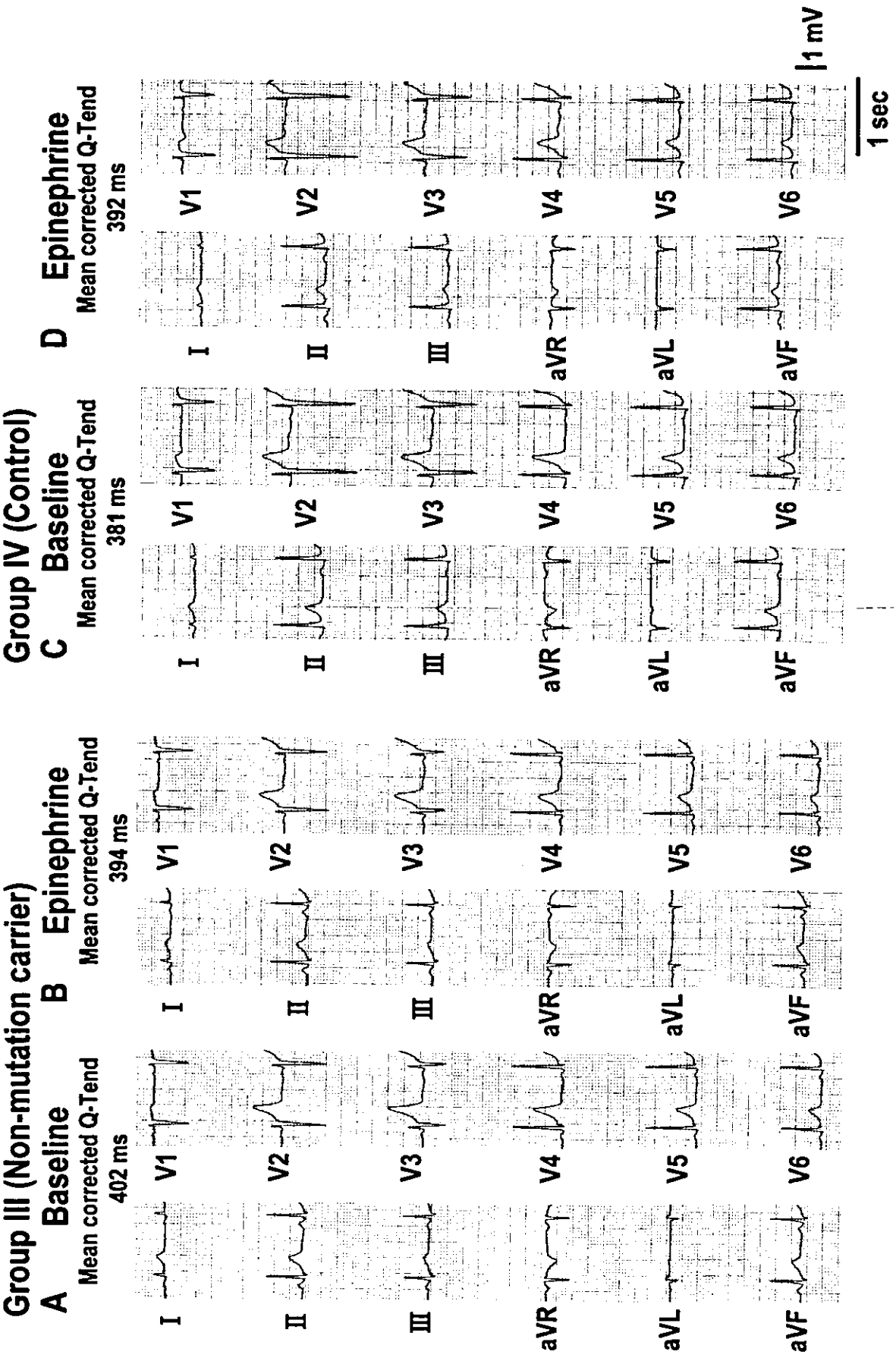

Figure 3. Twelve-lead electrocardiograms under baseline conditions and during epinephrine infusion in Group III (**A and B**) and Group IV (**C and D**) patients. No significant changes were produced by epinephrine in both Group III (402→394 ms) and Group IV (381→392 ms) patients.

genetic bases of the disease were known (12). These initial observations were based on the evidence that syncopal events could occur among family members with a "normal" QT interval. Several years later, Vincent et al. (13) reported that five (6%) of 82 mutation carriers from three LQT1 families had a normal QT interval. More recently, Priori et al. (5) have demonstrated a very low penetrance (38%, 9/24) in nine families with only one individual clinically affected with LQTS. In the present study, the average penetrance was 59% (20/34) among 11 LQT1 families. The sensitivity and specificity for identifying mutation carriers were 59% and 100% by using the electrocardiographic diagnostic criteria or when an LQTS score ≥2 was used, and they were 53% and 100% when a score ≥4 was used. Our data are in agreement with other reports demonstrating a 100% specificity and 53% sensitivity for diagnosis of high probability of LQTS (14). Overall, these findings strongly point to the need of novel tools to unveil nonpenetrant mutation carriers of LQTS.

Usefulness of epinephrine infusion in unmasking LQT1 mutation carriers. Provocative tests using catecholamine or exercise testing have long been considered to unmask some forms of congenital LQTS (6). Recent preliminary data by Ackerman et al. (8) have suggested the usefulness of an epinephrine test to unveil concealed LQT1 syndrome. This study provides systematic evaluation of the efficacy of epinephrine provocative challenge to unmask silent forms of LQTS in a group of genetically characterized individuals. Our data demonstrate that intravenous administration of epinephrine significantly improves the sensitivity of electrocardiographic diagnosis of LQTS in carriers of *KCNQ1* defects. Because *KCNQ1* is one of the two most common forms of congenital LQTS, this provocative challenge could be applied to a large number of individuals suspected to be affected by this variant of the disease. On the basis of current data, probands of congenital LQTS who had cardiac events during exercise and emotion (4), and particularly during swimming (2,3), have a high probability of being affected by *KCNQ1* genetic defects. Accordingly, all their family members become likely candidates for epinephrine provocative challenge. The identification of affected individuals with normal electrocardiographic phenotype is of major importance, as it would enable limiting exposure of these individuals to potentially dangerous conditions such as participation in competitive sports and use of drugs known to prolong repolarization, thus reducing the risk of life-threatening cardiac arrhythmias (15). However, it goes without saying that an epinephrine provocative test should only be done by cardiologists under enough preparation of intravenous beta-blockers as well as a direct cardioverter for unintentionally induced ventricular fibrillation. Darbar et al. (16) reported that the QTc was increased in lead II (but not in lead V_3) by epinephrine infusion even in normal controls, and suggested that this was due to increasing calcium current as well as hypokalemia induced by epinephrine. In this study, the QTce was not prolonged by epinephrine in Group III (nonmutation carrier) and Group IV (controls), probably as a result of the measurement of averaged QTce among all 12-leads as well as too-short epinephrine infusion (<5 min) to induce hypokalemia (17).

Mechanism of influence of epinephrine in LQT1 mutation carriers. Both experimental and clinical studies have suggested a differential response of action potential duration (APD) and QT interval to sympathetic stimulation among LQT1, LQT2, and LQT3 (7,8,18). Persistent and paradoxical prolongation of APD and QT interval at steady-state conditions of catecholamines was reported in LQT1 syndrome. Under normal conditions, beta-adrenergic stimulation is expected to increase net outward repolarizing current, owing to larger increase of outward currents, including Ca^{2+}-activated slow component of the delayed rectifier potassium current (I_{Ks}) and Ca^{2+}-activated chloride current, than that of an inward current, Na^+/Ca^{2+} exchange current ($I_{Na\text{-}Ca}$), resulting in an abbreviation of APD and QT interval. A defect in I_{Ks} in the LQT1 syndrome could account for failure of beta-adrenergic stimulation to abbreviate APD and QT interval, resulting in a persistent and paradoxical QT prolongation under sympathetic stimulation (18). In LQT2 syndrome, catecholamines are reported to initially prolong but then abbreviate APD and QT interval, probably because of an initial augmentation of $I_{Na\text{-}Ca}$ and a subsequent stimulation of I_{Ks}. In contrast to the LQT1 and LQT2 syndromes, catecholamines are reported to constantly abbreviate APD and QT interval as a result of a stimulation of I_{Ks} in the LQT3 syndrome, because an inward late sodium current (I_{Na}) was augmented in this genotype. Taken together with the data in the present study, the epinephrine test may be applied not only for unmasking silent mutation carriers with LQT1 syndrome but also for predicting genotype.

Symptomatic versus asymptomatic mutation carriers. In this study, the mean QTce, QTcp, and Tcp-e under the baseline conditions were significantly greater in the 15 symptomatic patients than in the 19 asymptomatic mutation carriers, consistent with previous large family studies without molecular diagnosis (12,19). Moreover, the epinephrine-induced prolongation of the mean QTce was significantly larger in the 15 symptomatic patients. This indicates a higher vulnerability of ventricular repolarization to sympathetic stimulation in symptomatic patients, although unknown factors may influence this phenomenon. The data also suggest that the epinephrine test may detect high-risk mutation carriers by the degree of QTc prolongation. In reverse, epinephrine-induced QTc prolongation was smaller in asymptomatic mutation carriers, indicating that the epinephrine test does not exert as great an effect to unveil mutation carriers in asymptomatic family members. However, epinephrine-induced prolongation of the mean QTce was >30 ms in all but two asymptomatic mutation carriers, and was clearly greater than those in either nonmutation carriers or normal controls. Prospective study using 30-ms cutoff with epinephrine challenge will be

needed in order to conclude the diagnostic value of the epinephrine test.

Dispersion of repolarization. The mean QTce was the most sensitive parameter to epinephrine; however, the mean Tcp-e was also increased by epinephrine only in the mutation carriers, suggesting that sympathetic stimulation increases transmural dispersion of repolarization (20), leading to arrhythmogenesis in the LQTS with *KCNQ1* defects. In contrast, the dispersion of the QTce, as an index of spatial dispersion of repolarization, was not significantly increased by epinephrine in Groups I and II (mutation carriers), and the changes in the dispersion of the QTce with epinephrine were not different among the four groups. These data may be explained by a recent elegant study using computer simulation conducted by Burnes et al. (21), in which they suggested that regional heterogeneity of repolarization was not reflected in QT dispersion recorded from the body surface ECG.

Study limitations. First, the numbers of families and of individuals in the present study are relatively small, and all patients are the same ethnic origin (Japanese). Because the issue of ethnicity as a modulator of genetically determined disease is receiving increasing attention, our data may or may not be applicable to other ethnicities.

Second, although peak of the T-wave was defined as that of the dominant T deflection when the T-wave had a biphasic or a notched configuration, it is still unclear which peak of the biphasic or notched T-wave reflects the repolarization of epicardial action potential. Further basic studies will be needed to conclude the cellular basis for complex T-waves.

Third, we used Bazett's formula for correction of heart rate. Bazett's formula is derived from normal individuals, and its use at higher heart rate is likely to lead to an overestimation of the QTc, thus contributing to the increase in sensitivity, which should be taken into account to interpret data in this kind of study.

Acknowledgments

We are indebted to Drs. Peter J. Schwartz and Arthur J. Moss for their critical review and insightful comments for the manuscript. We gratefully acknowledge the expert statistical assistance of Nobuo Shirahashi, Novartis Parma Co., and Yasuko Tanabe.

Reprint requests and correspondence: Dr. Wataru Shimizu, Division of Cardiology, Department of Internal Medicine, National Cardiovascular Center, 5-7-1 Fujishiro-dai, Suita, Osaka 565-8565, Japan. E-mail: wshimizu@hsp.ncvc.go.jp.

REFERENCES

1. Zareba W, Moss AJ, Schwartz PJ, et al. Influence of the genotype on the clinical course of the long-QT syndrome. N Engl J Med 1998; 339:960–5.
2. Moss A J, Robinson JL, Gessman L, et al. Comparison of clinical and genetic variables of cardiac events associated with loud noise versus swimming among subjects with the long QT syndrome. Am J Cardiol 1999;84:876–9.
3. Ackerman MJ, Tester DJ, Porter CJ, Edwards WD. Molecular diagnosis of the inherited long-QT syndrome in a woman who died after near-drowning. N Engl J Med 1999;341:1121–5.
4. Schwartz PJ, Priori SG, Spazzolini C, et al. Genotype-phenotype correlation in the long-QT syndrome: gene-specific triggers for life-threatening arrhythmias. Circulation 2001;103:89–95.
5. Priori SG, Napolitano C, Schwartz PJ. Low penetrance in the long-QT syndrome. Clinical impact. Circulation 1999;99:529–33.
6. Schechter E, Freeman CC, Lazzara R. After depolarizations as a mechanism for the long QT syndrome: electrophysiologic studies of a case. J Am Coll Cardiol 1984;3:1556–61.
7. Noda T, Takaki H, Kurita T, et al. Gene-specific response of dynamic ventricular repolarization to sympathetic stimulation in LQT1, LQT2 and LQT3 forms of congenital long QT syndrome. Eur Heart J 2002;23:975–83.
8. Ackerman MJ, Khositseth A, Tester DJ, Hejlik JB, Shen WK, Porter CB. Epinephrine-induced QT interval prolongation: a gene-specific paradoxical response in congenital long QT syndrome. Mayo Clin Proc 2002;77:413–21.
9. Keating M, Atkinson D, Dunn C, Timothy K, Vincent GM, Leppert M. Linkage of a cardiac arrhythmia, the long QT syndrome, and the Harvey ras-1 gene. Science 1991;252:704–6.
10. Schwartz PJ, Moss AJ, Vincent GM, Crampton RS. Diagnostic criteria for the long QT syndrome: an update. Circulation 1993;88:782–4.
11. Zhang L, Timothy KW, Vincent GM, et al. Spectrum of ST-T-wave patterns and repolarization parameters in congenital long-QT syndrome: ECG findings identify genotypes. Circulation 2000;102:2849–55.
12. Moss AJ, Schwartz PJ, Crampton RS, et al. The long QT syndrome: prospective longitudinal study of 328 families. Circulation 1991;84: 1136–44.
13. Vincent GM, Timothy KW, Leppert M, Keating MT. The spectrum of symptoms and QT intervals in carriers of the gene for the long-QT syndrome. N Engl J Med 1992;327:846–52.
14. Swan H, Saarinen K, Kontula K, Toivonen L, Viitasalo M. Evaluation of QT interval duration and dispersion and proposed clinical criteria in diagnosis of long QT syndrome in patients with a genetically uniform type of LQT1. J Am Coll Cardiol 1998;32:486–91.
15. Napolitano C, Schwartz PJ, Brown AM, et al. Evidence for a cardiac ion channel mutation underlying drug-induced QT prolongation and life-threatening arrhythmias. J Cardiovasc Electrophysiol 2000;11:691–6.
16. Darbar D, Smith M, Morike K, Roden DM. Epinephrine-induced changes in serum potassium and cardiac repolarization and effects of pretreatment with propranolol and diltiazem. Am J Cardiol 1996;77: 1351–5.
17. Brown MJ, Brown DC, Murphy MB. Hypokalemia from beta2-receptor stimulation by circulating epinephrine. N Engl J Med 1983;309:1414–9.
18. Shimizu W, Antzelevitch C. Differential response to beta-adrenergic agonists and antagonists in LQT1, LQT2 and LQT3 models of the long QT syndrome. J Am Coll Cardiol 2000;35:778–86.
19. Moss AJ, Zareba W, Hall WJ, et al. Effectiveness and limitations of beta-blocker therapy in congenital long-QT syndrome. Circulation 2000;101:616–23.
20. Shimizu W, Tanabe Y, Aiba T, et al. Differential effects of beta-blockade on dispersion of repolarization in absence and presence of sympathetic stimulation between LQT1 and LQT2 forms of congenital long QT syndrome. J Am Coll Cardiol 2002;39:1984–91.
21. Burnes JE, Ghanem RN, Waldo AL, Rudy Y. Imaging dispersion of myocardial repolarization, I: comparison of body-surface and epicardial measures. Circulation 2001;104:1299–305.

CARDIOVASCULAR MEDICINE

Abnormal response to sodium channel blockers in patients with Brugada syndrome: augmented localised wall motion abnormalities in the right ventricular outflow tract region detected by electron beam computed tomography

M Takagi, N Aihara, S Kuribayashi, A Taguchi, T Kurita, K Suyama, S Kamakura, M Takamiya

Heart 2003;**89**:169–174

See end of article for authors' affiliations

Correspondence to: Dr Naohiko Aihara, Division of Cardiology, Department of Internal Medicine, National Cardiovascular Centre, 5-7-1 Fujishiro-dai, Suita, Osaka 5658565, Japan; naihara@hsp.ncvc.go.jp

Accepted 18 September 2002

Objective: To investigate the relation between the wall motion abnormalities and sodium channel abnormalities in cases of the Brugada syndrome.
Design: Consecutive prospective case–control study in a single hospital.
Setting: Tertiary referral centre.
Patients: 13 consecutive patients with Brugada syndrome and 13 age and sex matched control subjects.
Interventions: Each subject underwent electron beam computed tomography (EBT) and a 12 lead ECG before and after disopyramide injection.
Main outcome measures: QRS width and the magnitude of ST segment elevation in the 12 lead ECG; wall motion by EBT.
Results: After disopyramide, EBT revealed deterioration of focal wall motion abnormalities in the right ventricular outflow tract region in eight of the 13 patients (62%). Prolongation of the QRS width after disopyramide injection in lead V2, which usually reflects the electrical activity in right ventricular outflow tract region, was greater in these eight patients ($p < 0.01$) than in the other five patients, in whom wall motion did not change after disopyramide. The degree of augmentation of ST segment elevation did not differ significantly between the two groups
Conclusions: The deterioration of wall motion abnormalities in the right ventricular outflow tract region after disopyramide suggests the presence of functional abnormalities of the sodium channel. Some patients with Brugada syndrome may have arrhythmogenic substrates with abnormal responses to sodium channel blockers.

The Brugada syndrome is associated with a high risk of sudden death.[1 2] Several antiarrhythmic agents (sodium channel blockers) are known to modulate ST segment elevation in patients with this syndrome.[2–5] Moreover, Chen and colleagues found mutations in the cardiac sodium channel gene, SCN5A, the first gene to be linked with Brugada syndrome, in three families.[6] However, the aetiology and arrhythmogenic substrate in this syndrome remain unknown.

Brugada syndrome is believed to occur in individuals with no apparent heart disease. The diagnosis of a structurally normal heart is based on the clinical features and on the results of routine cardiac imaging (coronary angiography, left and right ventriculography, and echocardiography). However, some studies have revealed wall motion abnormalities of the right ventricle in patients with Brugada syndrome.[7–10] The relation between these abnormalities and the cardiac sodium channels remains unknown.

Electron beam computed tomography (EBT) is a relatively new and sensitive imaging technique useful in diagnosing several features of arrhythmogenic right ventricular dysplasia[11 12] and Brugada syndrome.[8] We used EBT to determine whether a class IA sodium channel blocker modulated wall motion in patients with Brugada syndrome, and to explore the relation between the change in wall motion and changes in the characteristics of the 12 lead ECG after drug treatment.

METHODS

Patients

We used a patient–control design. Thirteen consecutive patients with Brugada syndrome admitted to our hospital between December 1998 and December 1999 and 13 controls were studied. The patients were eligible for inclusion in the study if they met all the following criteria:

- a history of syncope, cardiac arrest, or aborted sudden cardiac death with or without documentation of ventricular fibrillation
- no QT prolongation (corrected QT interval < 440 ms[-1])
- ST segment elevation (coved or saddleback type) in the precordial leads (V1 to V3) with or without right bundle branch block on the 12 lead ECG during sinus rhythm
- normal findings on physical examination
- no major abnormal findings of either right or left ventricular morphology or function demonstrated by chest radiography, echocardiography, and ventriculography
- no significant stenosis detected on coronary angiography.

All 13 patients were men. They ranged in age from 27–62 years (mean (SD), 46 (10) years) (table 1). None of the patients appear in our previous report.[8]

The control population consisted of eight age and sex matched healthy volunteers with normal hearts and normal

Table 1 Clinical characteristics of patients with the Brugada syndrome

Patient number	Age (years)	Documented VF	ECG findings during sinus rhythm: QRS in lead V2 (ms)	Qtc (ms^{-1})	RBBB	ST elevation (max, mm)	Electrophysiology: HV interval (ms)	Induced VF (pacing site)
Deteriorated group								
1	48	+	112	378	ICRBBB	V1–3 (7)	48	+ (RVOT)
2	33	+	132	376	CRBBB	V1,2 (1)	52	+ (RVOT)
3	39	–	96	370	–	V1–3 (4)	34	–
4	57	+	116	422	ICRBBB	V1,2 (1)	38	+ (RVOT)
5	62	+	96	408	–	V1–3 (1)	35	+ (RVOT)
6	49	+	100	380	ICRBBB	V1,2 (1)	35	+ (RVOT)
7	42	+	100	376	ICRBBB	V1,2 (1.6)	42	+ (RVOT)
8	56	+	108	411	ICRBBB	V1–3 (2)	40	+ (RV apex)
Unchanged group								
9	51	+	88	380	–	V1,2 (1.2)	32	+ (RVOT)
10	43	+	108	373	ICRBBB	V1,2 (2.5)	42	+ (RVOT)
11	51	+	100	420	ICRBBB	V1,2 (4)	38	+ (RVOT)
12	36	+	104	368	ICRBBB	V1–3 (3)	40	–
13	27	+	100	370	ICRBBB	V1–3 (2.8)	40	+ (RVOT)

CRBBB, complete right bundle branch block; HV, bundle of His to ventricle; ICRBBB, incomplete right bundle branch block; max, maximum; QTc, corrected QT interval; RBBB, right bundle branch block; RV, right ventricular; RVOT, right ventricular outflow tract; VF, ventricular fibrillation.

ECGs, and five age and sex matched volunteers with normal hearts but with right bundle branch block, for assessment of the wall motion. Controls ranged in age from 27–57 years (mean 45 (13) years). All controls had normal findings on physical examination and no abnormalities of right or left ventricular morphology or function on chest radiography and echocardiography.

Written informed consent was obtained from all patients and controls, and all underwent EBT and drug provocation testing, as well as an electrophysiological study.

Drug provocation testing

We examined the effects on the 12 lead ECG of a single dose of the class IA sodium channel blocker disopyramide (2 mg/kg), which was infused over 10 minutes in all patients and controls. The 12 lead ECG was recorded at double amplitude (2 cm/mV) and paper speed (50 mm/s) before and three minutes after the completion of the disopyramide infusion. The QRS onset and offset were determined visually in all 12 leads. The magnitude of the ST segment was measured visually at 20 ms after the end of the QRS in only lead V2 because we found that the maximum ST segment elevation occurred in this lead in all patients. We evaluated the change in the ST segment elevation in lead V2 and in the QRS width in all 12 leads.

CT scanning technique

Each subject underwent EBT with a C-150 scanner (Imatron, San Francisco, California, USA). We were able to obtain a near short axis oblique view of the heart with this instrument. Initially, we performed serial volume mode scanning at end systole as previously reported.[5] A total dose of 60 ml of non-ionic contrast medium (iopamidol, 370 mg I/ml; Nippon Schering, Osaka, Japan) was injected through the right antecubital vein with a mechanical injector. Using the multislice mode, eight-level scans were obtained with the injection of contrast medium to evaluate the function of both ventricles before and three minutes after completion of the disopyramide infusion, as previously reported.[5]

Assessment of morphological abnormalities

We evaluated the morphological and wall motion abnormalities visually by EBT. Each study was separately interpreted by two trained cardiologists and a radiologist who were blinded to the patient's clinical status.

We determined the wall thickness and aneurysmal change in both ventricles with volume mode scans, and evaluated any functional abnormalities (wall motion and wall thickening) in each of the chambers with movie mode scans. In the movie mode study, we compared the images before the disopyramide infusion with those obtained three minutes after the completion of the infusion. For visual semiquantitative right ventricular wall motion analysis, we made a 13 segment model of the right ventricle as previously reported.[4] For each segment, a score was assigned as follows: normal, 1; hypokinesis, 2; akinesis, 3; dyskinesis, 4. In all studies, focal hypokinesis, akinesis, and dyskinesis were defined, respectively, as decreased systolic excursion, no systolic excursion of a wall segment, and paradoxical motion of a wall segment compared with neighbouring segments, as assessed visually. Deterioration of the wall motion after the disopyramide infusion was defined as a greater decrease or disappearance of the segmental wall motion than before disopyramide. Diffuse deterioration of the wall motion was excepted because it probably represents the negative inotropic effect of disopyramide. Abnormalities were considered to be present if they were observed by two of the three observers. The sum of the wall motion scores for each subject was assessed to determine interobserver and intraobserver variabilities. Intraobserver variability was determined from triplicate measurements. Interobserver variability was determined from measurements by three observers.

We divided the patients into two groups (table 1): a *deteriorated group*, consisting of patients with deterioration of the wall motion after the disopyramide infusion (n = 8), and an *unchanged group*, consisting of patients with no deterioration of the wall motion (n = 5). We compared the 12 lead ECG characteristics before and after the disopyramide infusion in these two groups of patients.

Electrophysiological studies

All patients underwent electrophysiological studies in the non-sedated state. All antiarrhythmic drugs were discontinued for at least five drug half lives before the test. A 6 French steerable quadripolar electrode catheter with 2.5 mm interelectrode spacing (EP Technologies Inc, Sunnyvale, California, USA) was introduced percutaneously through the femoral vein and positioned in the right ventricle under fluoroscopic guidance. Bipolar electrograms were recorded at more than 10 sites in the right ventricle. Abnormal bipolar electrograms were considered to be those with a low amplitude (< 1 mV) or long duration (> 70 ms), or both.

Programmed electrical ventricular stimulation was achieved using a 2 ms pulse duration at twice the diastolic threshold, delivered from a programmable stimulator (SEC-3120, Nihon Kohden, Tokyo, Japan). The protocol included an

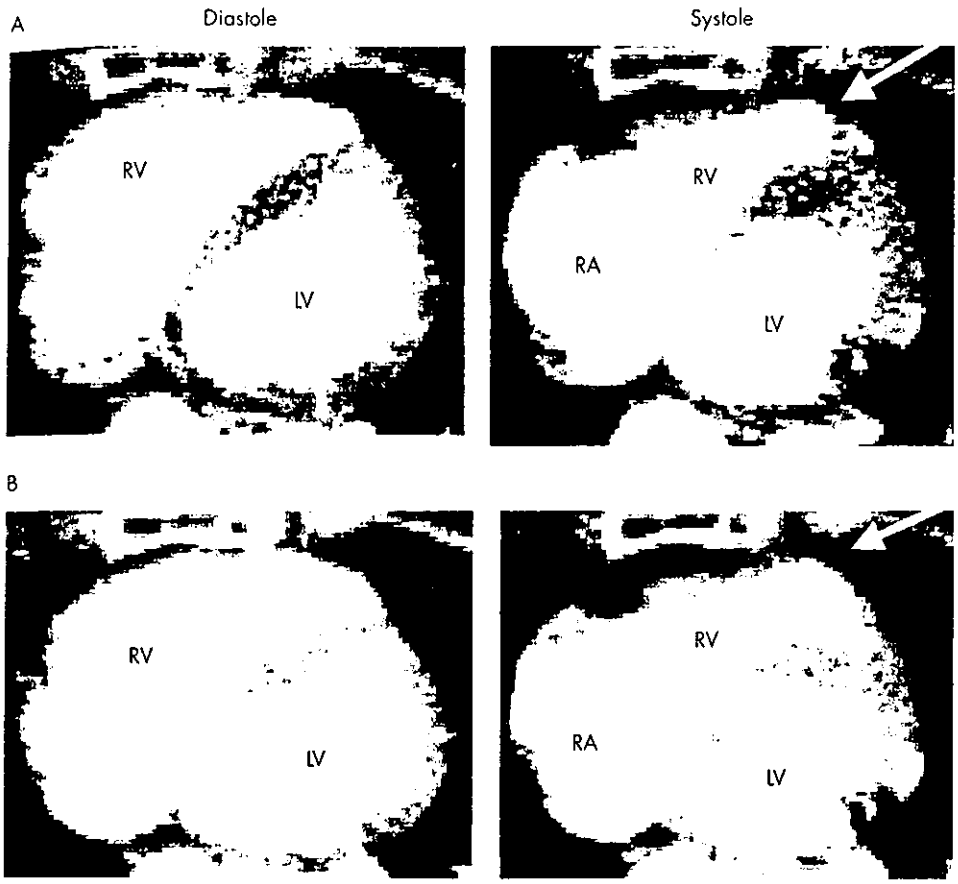

Figure 1 Representative electron beam computed tomography findings in a patient with Brugada syndrome in the "deteriorated" group (see text for definition of groups). A "near short axis" movie mode scan (acquisition time, 50 ms) was obtained with the administration of contrast medium. (A) Wall motion abnormalities were observed before the disopyramide infusion in the right ventricular outflow tract region (arrowhead). (B) The wall motion abnormalities were impaired after the disopyramide infusion (arrowhead). LA, left atrium; LV, left ventricle; RA, right atrium; RV, right ventricle.

eight beat ventricular paced drive train at two basic cycle lengths (500 and 400 ms), followed by decremental introduction of up to triple extrastimuli at the right ventricular apex and right ventricular outflow tract. The end point was either reproducible induction of ventricular fibrillation or completion of the pacing protocol.

Statistics

Data are presented as mean (SD). Comparison of absolute values of QRS width and ST segment elevation before and after the disopyramide infusion in the two groups was done using repeated measures two way analysis of variance (ANOVA). Comparison of the difference (Δ) in the QRS duration and ST segment elevation before and after the disopyramide infusion was done using one way ANOVA with a multiple comparison test. Assessments of the interobserver and intraobserver variability were also undertaken using the Bland and Altman method. Probability values of $p < 0.05$ were taken as significant.

RESULTS

The characteristics of the two groups of patients are presented in table 1. None of the patients were related. Their mean age was 48 (10) years in the deteriorated group and 42 (10) years in the unchanged group (NS). Of the patients in the deteriorated group, two had a normal QRS duration, five had incomplete right bundle branch block, and one had complete right bundle branch block. Of the patients in the unchanged group, one had a normal QRS duration and four had incomplete right bundle branch block. All 13 patients had several syncopal episodes with palpitations or aborted sudden cardiac death. Ventricular fibrillation had been documented in 10 of these patients on ECG recordings. The mean age of the controls with or without right bundle branch block was 47 (10) and 43 (12) years, respectively (NS). None of controls had a history of syncopal attacks.

Morphological assessment: assessment of the right ventricle

EBT findings in patients with Brugada syndrome

Before the disopyramide infusion, EBT showed wall motion abnormalities of the right ventricle in nine (69%) of the 13 patients. All these abnormalities were in the anterior basal region of the right ventricular outflow tract (fig 1A). There were no abnormal findings in relation to wall thickness or the focal presence of intramural or transmural fatty tissue.

After the disopyramide infusion, there was deterioration in wall motion in eight patients (fig 1B). In two of them, the abnormalities were found only after the disopyramide infusion (fig 2). The sites of deterioration in the wall motion abnormalities were limited at the anterior base of the right ventricular outflow tract region. None of the patients in the unchanged group had diffuse deterioration of wall motion after the disopyramide infusion.

EBT findings in the control subjects

None of the controls, with or without right bundle branch block, had abnormal findings in relation to wall thickness or the focal presence of fatty tissue on static images. In none of the controls were there wall motion abnormalities or deterioration of the wall motion after the disopyramide infusion.

Morphological assessment: assessment of the left ventricle

No abnormal left ventricular findings were observed in any of the patients with Brugada syndrome or in the control subjects, either before or after the disopyramide infusion. There were no significant differences in either interobserver or intraobserver variability between the two groups of patients and the controls.

Twelve lead ECG findings

QRS duration in patients with Brugada syndrome

The mean QRS durations before and after the disopyramide infusion in the 13 patients with Brugada syndrome are

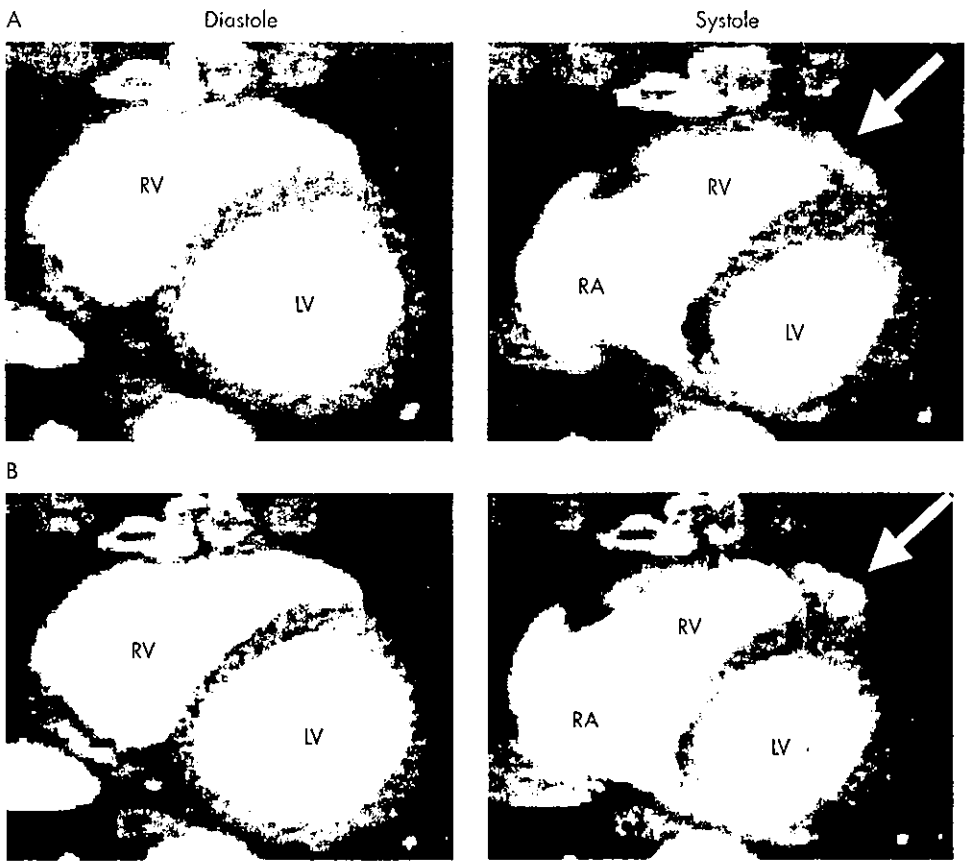

Figure 2 Representative electron beam computed tomography findings in a patient in the "deteriorated" group (see text for definition of the groups) without wall motion abnormalities before the disopyramide infusion (A, arrowhead). The wall motion abnormalities were unmasked after the disopyramide infusion (B, arrowhead). LA, left atrium; LV, left ventricle; RA, right atrium; RV, right ventricle.

presented in table 2. No significant difference between the two groups was present in any lead. After the disopyramide infusion, the mean QRS duration increased in both groups in all the leads ($p < 0.05$). In lead V2 only, the mean difference in the QRS duration compared with the pre-disopyramide value (mean ΔQRS duration) was larger in the deteriorated group than in the unchanged group (23 (5) *v* 10 (3) ms, respectively; $p = 0.0001$) (table 3). Representative ECG findings are shown in fig 3.

ST segment elevation in lead V2 in patients with Brugada syndrome

Under control conditions, all patients showed ST segment elevation (coved or saddleback type in precordial leads V1–V3) during sinus rhythm. The maximum ST segment elevation occurred in lead V2. The mean ST segment elevation before disopyramide was 0.28 (0.24) mV in the deteriorated group and 0.27 (0.10) mV in the unchanged group. After disopyramide, the magnitude of the ST segment elevation increased in all patients ($p = 0.001$). Mean ST segment elevation after disopyramide was 0.51 (0.35) mV in the deteriorated group and 0.41 (0.08) mV in the unchanged group. There was no significant difference between the two groups in this variable.

The mean difference in the magnitude of the ST segment elevation before and after the disopyramide infusion (mean ΔST) was 0.24 (0.12) mV in the deteriorated group and 0.14 (0.07) mV in the unchanged group. The difference was greater in the patients in the deteriorated group than in those in the unchanged group, but this did not reach significance ($p = 0.15$). Representative ECG findings are shown in fig 3.

QRS duration and ST segment elevation in the control subjects without right bundle branch block

The mean QRS duration before disopyramide in the controls without right bundle branch block was less than in the

Table 2 QRS duration before and after disopyramide infusion

Lead	Before disopyramide		After disopyramide		Statistics (p value)		
	Deteriorated (n=8) (ms)	Unchanged (n=5) (ms)	Deteriorated (n=8) (ms)	Unchanged (n=5) (ms)	Group factor	Drug factor	Interaction
I	96 (25)	86 (10)	118 (31)	96 (8)	0.23	<0.01*	0.12
II	111 (25)	105 (17)	124 (29)	112 (11)	0.53	0.03*	0.53
III	103 (16)	110 (14)	115 (18)	121 (8)	0.41	<0.01*	0.94
aVR	104 (27)	101 (16)	119 (26)	113 (15)	0.74	<0.01*	0.54
aVL	107 (27)	94 (17)	110 (27)	105 (16)	0.47	<0.01*	0.06
aVF	111 (27)	111 (17)	122 (27)	116 (9)	0.84	<0.01*	0.20
V1	114 (16)	104 (12)	128 (14)	114 (12)	0.14	<0.01*	0.56
V2	108 (13)	100 (8)	131 (15)	110 (7)	0.06	<0.01*	<0.01*
V3	117 (16)	106 (9)	132 (13)	114 (10)	0.06	<0.01*	0.07
V4	117 (22)	102 (10)	131 (20)	113 (7)	0.14	<0.01*	0.53
V5	109 (21)	103 (15)	123 (18)	111 (12)	0.39	<0.01*	0.21
V6	104 (21)	102 (15)	120 (25)	112 (14)	0.68	<0.01*	0.31

Values are mean (SD).
*Significant difference before and after disopyramide

Table 3 Difference in QRS duration before and after disopyramide infusion (ΔQRS duration)

Lead	Deteriorated group (n=8) (ms)	Unchanged group (n=5) (ms)	p Value
I	18 (11)	12 (10)	0.52
II	11 (10)	9 (6)	0.30
III	11 (6)	12 (9)	0.14
aVR	15 (9)	13 (9)	0.13
aVL	9 (4)	8 (3)	0.23
aVF	12 (9)	9 (3)	0.28
V1	13 (8)	12 (10)	0.08
V2	23 (5)	10 (3)	<0.01
V3	15 (7)	8 (5)	0.13
V4	13 (10)	12 (3)	0.17
V5	14 (8)	9 (8)	0.51
V6	13 (6)	12 (3)	0.62

Values are mean (SD).

patients with Brugada syndrome in all leads ($p < 0.05$). None of the control subjects had either pronounced ST segment elevation (more than 0.16 (0.02) mV in lead V2) or QTc prolongation (more than 377 (13) $ms^{1/2}$ in lead V2) under control conditions.

After the disopyramide infusion, the patients in the unchanged group showed a larger mean ΔQRS duration ($p = 0.17$ in lead V2) and a larger mean ΔST than the control subjects. However, there were no significant difference in these variables between the patients in the unchanged group and the control subjects in any lead.

Electrophysiological study

No abnormal bipolar electrograms were recorded in the right ventricle in any patient. The mean HV intervals were 41 (7) ms and 38 (4) ms in the deteriorated group and unchanged group, respectively (NS). Ventricular fibrillation was induced in seven patients (88%) in the deteriorated group and in four patients (80%) in the unchanged group (NS) by double or triple extrastimuli from the right ventricular apex or outflow tract region (table 1).

DISCUSSION

Our findings show that wall motion abnormalities of the anterior base of the right ventricular outflow tract region can be detected in a substantial number (69%) of patients with Brugada syndrome using EBT under control conditions. Eight of our 13 patients with this syndrome had further deterioration of the wall motion in the anterior basal region of the right ventricular outflow tract after the disopyramide infusion. In two of these eight patients, the wall motion abnormalities were unmasked after the disopyramide infusion. We also found that patients with deterioration in wall motion after disopyramide had significant prolongation of QRS duration and a larger change in QRS duration in lead V2—which reflects the electrical activity of the right ventricular outflow tract region—than the patients with no impairment of wall motion after disopyramide. Thus we found that patients with the Brugada syndrome show heterogeneity of response to sodium channel blockers, and that the area with this heterogeneous response is in the right ventricular outflow tract region.

Although Brugada and colleagues found no clear underlying heart disease in their patients and proposed that the cause of the syndrome was an electrical disorder,[1] some other studies[7–10] have reported wall motion abnormalities of the right ventricle in patients with the Brugada syndrome. Martini and colleagues found morphological and wall motion abnormalities of the right ventricle in five of six patients, and observed right ventricular enlargement, significant fibrous adipose replacement in the free wall, and fibrosis of the bifurcating bundle and proximal bundle branches in one necropsy case.[7] Corrado and associates reported that four of seven members of a family affected by the syndrome, and in whom characteristics including right bundle branch block, ST segment elevation, and sudden cardiac death were observed, had structural abnormalities of the right ventricle on echocardiography.[8] A recent study carried out by us using EBT[4] showed that patients with Brugada syndrome had a high incidence of wall motion abnormalities in the right ventricle, which suggest that this condition may be associated with underlying heart disease involving the right ventricle, especially the right ventricular outflow tract region. In some studies it has been found that class IA and IC sodium channel

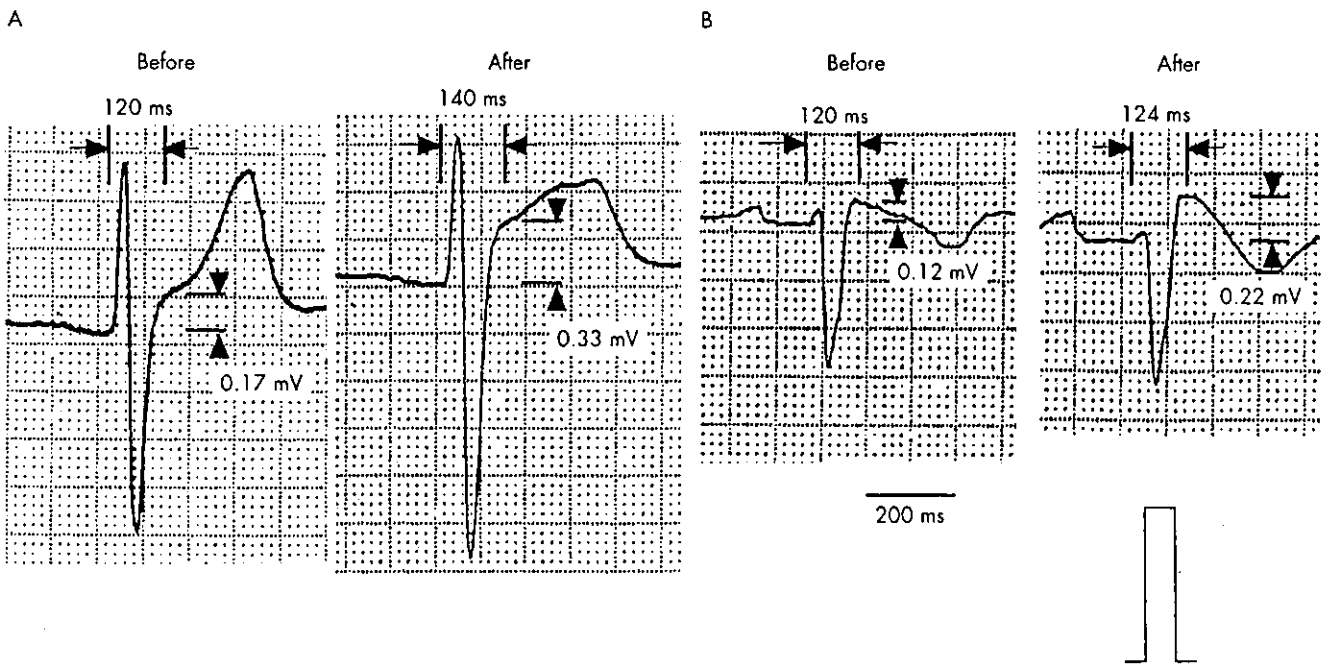

Figure 3 Representative lead V2 ECGs from patients with Brugada syndrome before and after the disopyramide infusion. The difference in the QRS duration and magnitude of the ST segment elevation of that observed before the disopyramide infusion with that after was significantly larger in the patients in the "deteriorated" group (A) than in those in the "unchanged" group (B) (see text for definition of the groups).

blockers may augment the ST segment elevation.[3-5] Moreover, some mutations in the cardiac sodium channel gene, SCN5A—a gene linked to Brugada syndrome—have recently been reported.[9 13]

In the present study, we found that some of our patients with Brugada syndrome showed further deterioration in wall motion in the right ventricular outflow tract region after disopyramide—that is, these patients may be more sensitive to sodium channel blockers in that area of the heart. As we found no wall motion abnormalities before or after disopyramide in the controls with right bundle branch block, we conclude that the observed abnormalities in wall motion are not caused by asynchrony of depolarisation but are specific to the Brugada syndrome. We suggest that in these patients the deterioration in the wall motion abnormalities detected by EBT may be functional and may be related to sodium channel abnormalities.

We believe this is the first study to demonstrate a relation between wall motion abnormalities and an abnormal response to sodium channel blockers, and that sodium channel abnormalities may be present in the right ventricular outflow tract region in patients with the Brugada syndrome. Other patients with this syndrome but without deterioration in the wall motion after disopyramide also showed a longer mean ΔQRS duration and a larger mean ΔST than the control subjects. We therefore suggest that patients with Brugada syndrome are likely to have an abnormal response to sodium channel blockers, but that EBT revealed deterioration in the wall motion after disopyramide only in those patients who had severe sodium channel abnormalities.

In the six patients with wall motion abnormalities at baseline and with deterioration in wall motion after disopyramide, we speculate that the baseline abnormalities may be a manifestation of a depolarisation abnormality based on a sodium channel defect, or they might indicate underlying structural heart disease. In the three patients with wall motion abnormalities but no deterioration after disopyramide, we assume there may be underlying structural heart disease, but the aetiology of this remains unclear. As the number of such patients was so small, we need more data on similar cases for a better understanding of the aetiology of wall motion abnormalities unresponsive to disopyramide.

In our study, the mean difference in the magnitude of the ST segment before and after disopyramide was greater in the deteriorated group than in the unchanged group, but this difference was not significant. Some basic studies of experimental models of the Brugada syndrome have suggested that ST segment elevation is related to an increased transient outward current (I_{to}) in the right ventricular epicardium but not in the right ventricular endocardium.[14 15] Disopyramide has modest I_{to} blocking properties[16] and these could mask any differences in ST segment elevation.

Study limitations

Flecainide, a class Ic sodium channel blocker, is widely used in provocative testing to unmask the ECG phenotype of Brugada syndrome because of its strong use dependent blockade of the fast sodium current.[17 18] We initially used flecainide in a few of our patients; however, on EBT all these patients showed diffuse deterioration in wall motion after the infusion, probably because of the strong negative inotropic effect of this agent. Because of this, we were unable to assess the specific changes in wall motion abnormality. In the present study, therefore, we used disopyramide as a sodium channel blocker, because of its weaker negative inotropic effects.

We undertook genetic analyses on 10 patients but did not identify any genetic disorders. As the number of patients was so small, further data are needed for a better understanding of relation between gene mutation and focal wall motion abnormalities in patients with the Brugada syndrome.

In order to evaluate whether the presence or absence of the wall motion abnormalities observed has prognostic relevance, we need to collect prospective data on spontaneously occurring ventricular tachyarrhythmias.

Conclusions

Deterioration in wall motion abnormalities in the right ventricular outflow tract region after a disopyramide infusion suggests the presence of functional abnormalities of the sodium channel. This means that some patients with Brugada syndrome may have arrhythmogenic substrates with heterogeneous responses to sodium channel blockers in the right ventricular outflow tract region.

Authors' affiliations

M Takagi, N Aihara, S Kuribayashi, A Taguchi, T Kurita, K Suyama, S Kamakura, M Takamiya, Division of Cardiology, Department of Internal Medicine, National Cardiovascular Centre, Suita, Osaka, Japan

REFERENCES

1 **Brugada J**, Brugada R, Brugada P. Right bundle-branch block and ST-segment elevation in leads V1 through V3: a marker for sudden death in patients without demonstrable structural heart disease. *Circulation* 1998;**97**:457–60.
2 **Brugada J**, Brugada P. Further characterization of the syndrome of right bundle branch block, ST segment elevation, and sudden cardiac death. *J Cardiovasc Electrophysiol* 1997;**8**:325–31.
3 **Miyazaki T**, Mitamura H, Miyoshi S, *et al*. Autonomic and antiarrhythmic drug modulation of ST segment elevation in patients with Brugada syndrome. *J Am Coll Cardiol* 1996;**27**:1061–70.
4 **Krishman SC**, Josephson ME. ST segment elevation induced by class IC antiarrhythmic agents: Underlying electrophysiological mechanisms and insights into drug-induced proarrhythmia. *J Cardiovasc Electrophysiol* 1998;**9**:1167–72.
5 **Fujiki A**, Usui M, Nagasawa H, *et al*. ST segment elevation in the right precordial leads induced with class IC antiarrhythmic drugs: insights into the mechanism of Brugada syndrome. *J Cardiovasc Electrophysiol* 1999;**10**:214–18.
6 **Chen Q**, Kirsch GE, Zhang D, *et al*. Genetic basis and molecular mechanism for idiopathic ventricular fibrillation. *Nature* 1998;**392**:293–6.
7 **Martini B**, Nava A, Thiene G, *et al*. Ventricular fibrillation without apparent heart disease: description of six cases. *Am Heart J* 1989;**118**:1203–9.
8 **Takagi M**, Aihara N, Kuribayashi S, *et al*. Localized right ventricular morphological abnormalities detected by electron-beam computed tomography represent arrhythmogenic substrates in patients with Brugada syndrome. *Eur Heart J* 2001;**22**:1032–41.
9 **Corrado D**, Nava A, Buja G, *et al*. Familial cardiomyopathy underlies syndrome of right bundle branch block, ST segment elevation and sudden death. *J Am Coll Cardiol* 1996;**27**:443–8.
10 **Sato Y**, Kato K, Hashimoto M, *et al*. Localized right ventricular structural abnormalities in patients with idiopathic ventricular fibrillation: magnetic resonance imaging study. *Heart Vessels* 1996,**11**:100–3.
11 **Tada H**, Shimizu W, Ohe T, *et al*. Usefulness of electron-beam computed tomography in arrhythmogenic right ventricular dysplasia: relationship to electrophysiological abnormalities and left ventricular involvement. *Circulation* 1996,**94**:437–44.
12 **Hamada S**, Takamiya M, Ohe T, *et al*. Arrhythmogenic right ventricular dysplasia: evaluation with electron-beam CT. *Radiology* 1993;**187**:723–7.
13 **Makita N**, Shirai N, Wang DW, *et al*. Cardiac Na+ channel dysfunction in Brugada syndrome is aggravated by β-subunit. *Circulation* 2000;**101**:54–60.
14 **Antzelevitch C**, Yan GX, Shimizu W. Electrical heterogeneity, the ECG, and cardiac arrhythmias. In: Zipes DP, Jalife J, eds. *Cardiac electrophysiology: from cell to bedside*. Philadelphia: WB Saunders Co. 2000:222–38.
15 **Yan GX**, Antzelevitch C. Cellular basis for the electrocardiographic J wave. *Circulation* 1996;**93**:372–9.
16 **Virag L**, Varro A, Papp C. Effect of disopyramide on potassium currents in rabbit ventricular myocytes. *Naunyn Schmiedebergs Arch Pharmacol* 1998;**357**:268–75.
17 **Brugada R**, Brugada J, Anzelevitch C, *et al*. Sodium channel blockers identify risk for sudden death in patients with ST-segment elevation and right bundle branch block but structurally normal hearts. *Circulation* 2000;**101**:510–15.
18 **Priori SG**, Napolitano C, Schwartz PJ, *et al*. The elusive link between LQT3 and Brugada syndrome: the role of flecainide challenge. *Circulation* 2000,**102**:945–7.

Journal of Interventional Cardiac Electrophysiology 8, 129–133, 2003

Directions of Atrial Excitation Wavefront Influenced Antegrade Conduction of Manifest Accessory Atrioventricular Pathway: A Case Report

Takeshi Aiba, Takashi Kurita, Kazuhiro Suyama, Kazuhiro Satomi, Atsushi Taguchi, Wataru Shimizu, Naohiko Aihara, and Shiro Kamakura

Division of Cardiology, Department of Internal Medicine, National Cardiovascular Center, 5-7-1 Fujishiro-dai, Suita, Osaka, 565-8565, Japan

Abstract. **We report a case of left accessory atrioventricular pathway (AP) which antegrade conduction was manifest during pacing from the anterior site of the atrial insertion, but absent during pacing from the posterior site. Infusion of adenosine triphosphate during pacing from the posterior site induced a conduction block of atrioventricular node without affecting the persistent antegrade conduction block of the AP. These findings suggested that the different response of the AP according to the directional change of atrial conduction was not due to a 'linking' phenomenon, but may relate to the impedance mismatch because of an oblique fashion of the pathway.**

Key Words. **Wolff-Parkinson-White syndrome, conduction block, oblique accessory atrioventricular pathway**

Backgrounds

The past experimental study demonstrated that the conduction of atrial muscle fiber was blocked by the directional change of its propagation because of an abrupt increase in the effective axial resistivity [1]. However, there has never been reported about such phenomenon in a conduction of human antegrade accessory atrioventricular pathway (AP). We report a case of manifest left AP with an oblique course, which conduction was revealed during pacing from the anterior site of the atrial insertion, but completely absent during pacing from the posterior site.

Case Report

A 49-years female, who had a history of frequent palpitation because of orthodromic atrioventricular (AV) reciprocating tachycardia for 24 years, was admitted to our hospital for treatment of radiofrequency catheter ablation. The 12-lead ECG during sinus rhythm consisted with a pre-excitation of delta wave, which indicated a left anterolateral AP (Fig. 1A). Two 6-French catheters (EP Technologies, Mountain View, CA, USA) were placed under fluoroscopic guidance in the high right atrium and right ventricular apex, and a 6-French octapolar catheter (EP Technologies) was placed in His bundle position. A 2-French 16-electrodes catheter (Pathfinder^{TM}, Cardima, Benicia St, Fremont, CA) was inserted into coronary sinus via 5-French guiding catheter. A 7-French quadripolar catheter with a 4-mm tip electrode (Marinr^{TM}, Medtronic, Minneapolis, USA) was inserted via the right femoral artery and advanced retrogradely into the left ventricle for mapping the mitral annulus and ablation.

The delta wave could be manifested during pacing from the distal (anterior) pair (1–2 to 3–4) of the coronary sinus electrodes (Fig. 1B). The effective refractory period of the antegrade AP conduction was 390 msec when basic cycle length was 500 msec, and 1:1 conduction was maintained until 120 bpm. However, the delta wave was completely absent during pacing from the proximal (posterior) pair (5–6 to 15–16) of the coronary sinus electrodes at any cycle lengths and any coupling intervals (Fig. 1C). Moreover, these persistent antegrade AP conduction block could not be affected by AV node conduction block using a rapid infusion of adenosine triphosphate (Fig. 2). The atrioventricular simultaneous pacing with atrial pacing from the posterior pair of coronary sinus electrodes could not also reveal any antegrade AP conduction.

The earliest atrial activity during pacing from right ventricle was recognized at the anterolateral

Address for correspondence: Takashi Kurita, MD, PhD, Division of Cardiology, Department of Internal Medicine, National Cardiovascular Center, 5-7-1 Fujishiro-dai, Suita, Osaka, 565-8565, Japan.

Received 3 April 2002; accepted 8 November 2002

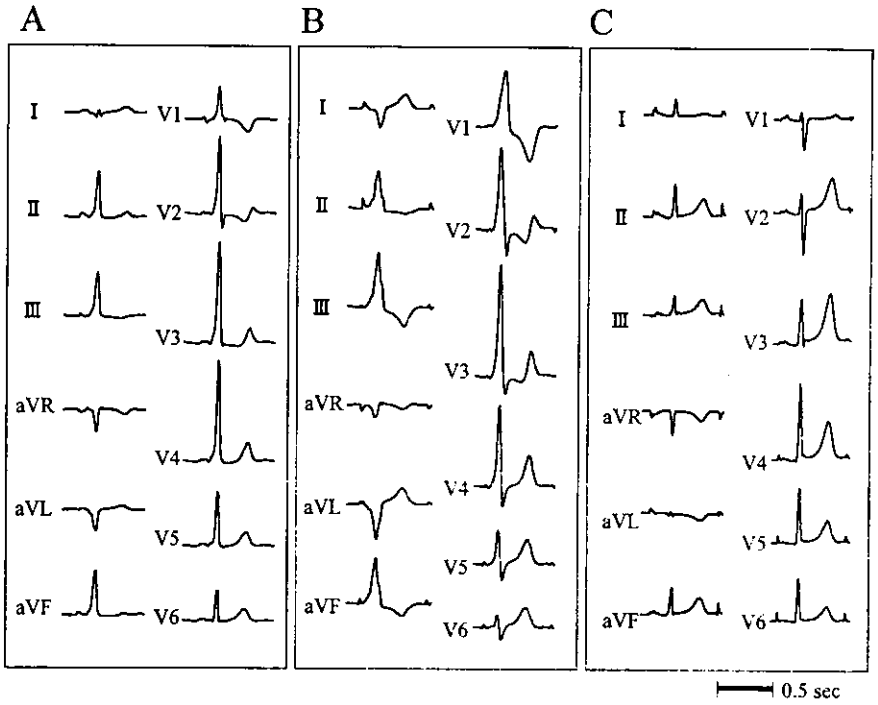

Fig. 1. 12-lead ECG during sinus rhythm and pacing from coronary sinus (CS) electrodes. The delta wave was manifested during sinus rhythm (A) and pacing from anterior (CS 3–4) pair of CS electrodes (B). However, the delta wave was absent during pacing from posterior (CS 5–6) pair of CS electrodes (C). These pacing were performed at basic cycle length of 600 ms.

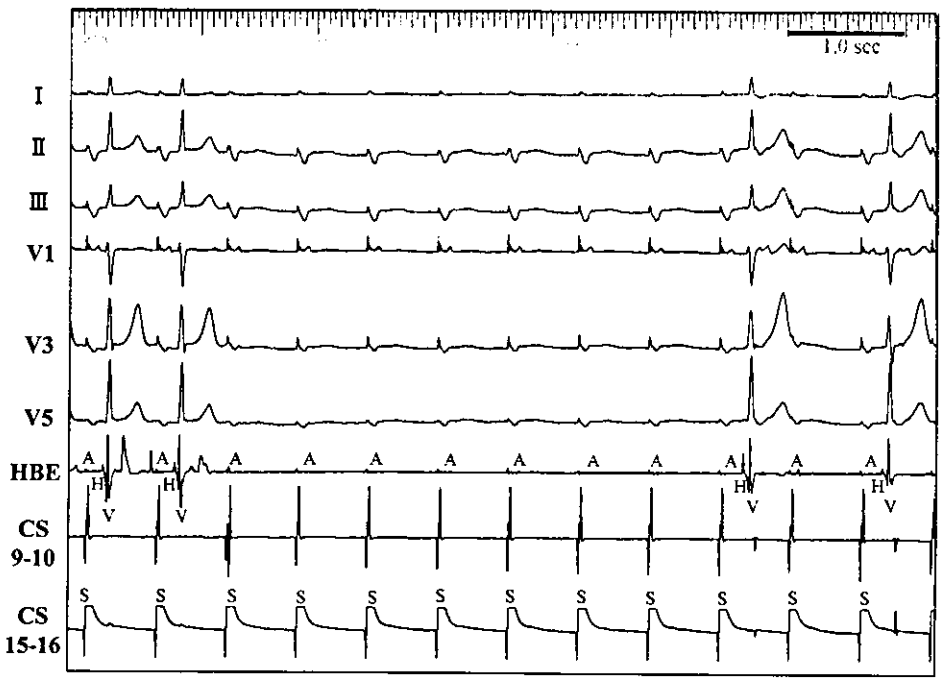

Fig. 2. The surface electrocardiograms and electroendocardial recordings during pacing from 15–16 pair of coronary sinus (CS) electrodes with an infusion of adenosine triphosphate, which made an atrioventricular node conduction block without revealing pre-excitation conduction. A = atrial potential, H = His bundle potential, V = ventricular potential, HBE = His bundle electrode.

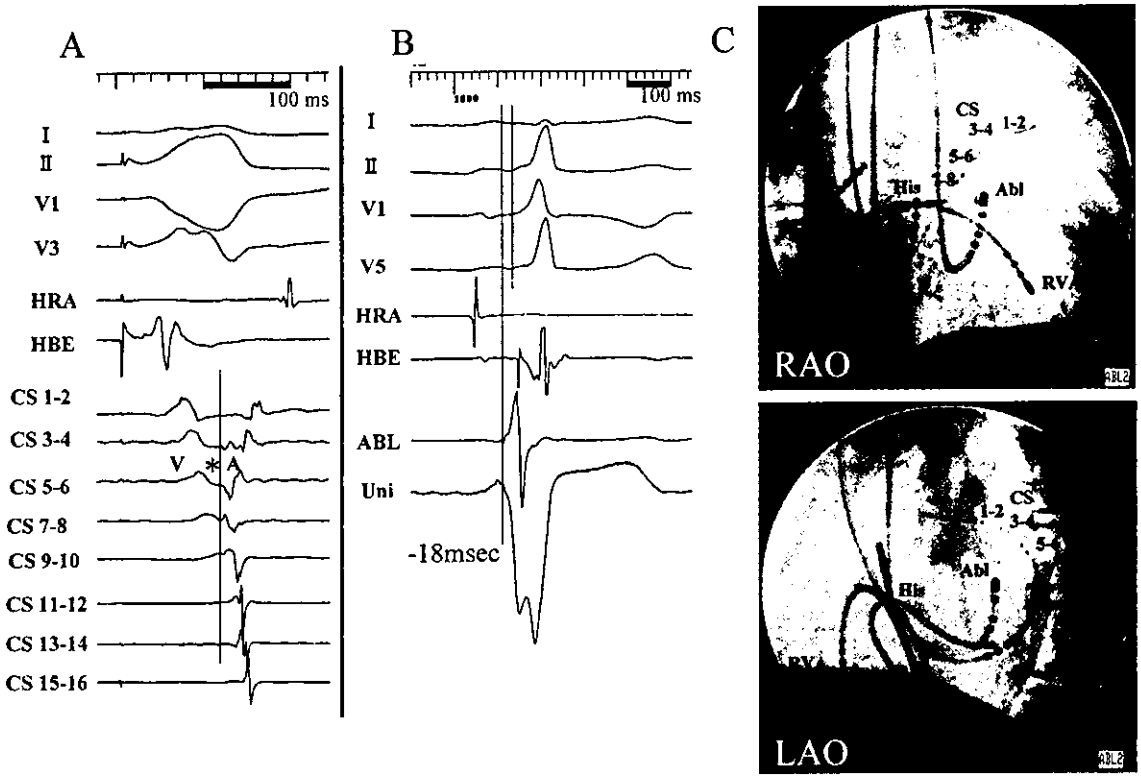

Fig. 3. The electroendocardial recording during pacing from right ventricle (A) and sinus rhythm (B), and position of catheters in right anterior oblique (RAO) 30° and left anterior oblique (LAO) 60° views (C). The earliest atrial activity during pacing from right ventricle was recognized at the anterolateral site in the coronary sinus (between the 3–4 and 5–6 pair of the coronary sinus electrodes). The earliest ventricular activity during sinus rhythm was preceded 18 msec to QRS complex with QS pattern in unipolar electrode (B), which catheter position was at the lateral site of mitral annulus (C). CS = coronary sinus, ABL = ablation catheter, Uni = unipolar electrode at distal of ablation catheter, RVA = right ventricular apex.

site in the coronary sinus (between the 3–4 and 5–6 pair of the coronary sinus electrodes) (Fig. 3A). The effective refractory period of the retrograde AP conduction was 270 msec when basic cycle length was 500 msec, and 1:1 conduction was maintained until 190 bpm. The characteristics of the antegrade and retrograde AP conduction had no decremental properties. On the other hand, detailed mapping of the ventricular site of the mitral annulus during sinus rhythm (Fig. 3B) demonstrated that the ventricular insertion of AP located at the lateral site (Fig. 3C). Although the rapid ventricular activation was not obtained around the mitral annuls, the onset of ventricular activity was earliest at this site (18 ms preceding the delta wave) . Moreover the unipolar electrode showed QS pattern. Thus, we decided this site to be the ventricular insertion of AP and a single radiofrequency application from this site could abolish the antegrade and retrograde AP conduction permanently. These findings suggested that the AP was single and its course might be a significantly oblique, which atrial insertion was located anterior to the ventricular insertion.

Discussion

This is the first report to demonstrate the antegrade AP in which conduction was depending on the direction of the atrial depolarization. In human AP, although many mechanisms were suggested in the intermittent AP conduction, the characteristics of this conduction depending on the direction of its propagation have never been reported.

The intermittent conduction has been frequently observed and suggested as an explanation for the variability of R-R intervals during atrial fibrillation in patients with Wolff-Parkinson-White syndrome. Previous studies demonstrated the mechanism of the concealed AP conduction and its presence by some atrial or ventricular pacing methods [2–8]. The reasons of the intermittent AP conduction was suggested such mechanisms as (1) gap phenomenon and supernormal conduction [4,5], (2) linking phenomenon [6], (3) peeling back phenomenon [7], (4) phase 3 or 4 block [8], (5) automatic tone [9], and (6) impedance mismatch. The AP conduction must be manifested at

some pacing intervals or infusion of isoproterenol in the functional block of (1)–(5) theories. However, in this patient, the antegrade AP conduction had never been revealed at any pacing intervals during pacing from the posterior side of the atrial insertion. Moreover, the atrioventricular simultaneous pacing with atrial pacing from the posterior pair of coronary sinus electrodes could not also reveal any antegrade AP conduction. On the other hand, pacing from the anterior side easily captured the AP. During pacing from these posterior pair of the coronary sinus electrode, an infusion of adenosine triphosphate made an AV node conduction block without revealing pre-excitation conduction. Thus, this latent AP conduction was not due to the gap phenomenon, supernormal conduction, peeling back phenomenon, phase 3 or 4 block, and linking phenomenon, but might be due to another reason like an impedance mismatch.

Spach et al. demonstrated that, using an experimental atrial model of a small fiber arising from a larger bundle at an acute angle, the conduction to the small fiber depended on the angle from which the excitation wavefront entered the fiber [1]. They suggested the atrial conduction might become slowly and blocked because of an abrupt increase in the effective axial resistivity in the direction of propagation. Goldberger et al. reported two patients with latent decremental AP in which conduction was manifest only during antidromic AV reentrant tachycardia [10]. They suggested the reason of its absence of pre-excitation in any situations without antidromic AV reentrant tachycardia was to be slowly and decremental conduction of the fiber. The fluoroscopic images (Fig. 3C) showed that this AP was the oblique course with its atrial insertion located anterior to the ventricular insertion. Otomo et al. reported that many APs were oriented with an oblique course with which atrial insertion was anterior to the ventricular insertion [11]. However, the conduction block depending on the direction of its propagation was not always observed in an oblique AP. The reason of this selective conduction block might be due to an abrupt increase in the effective axial resistivity in the direction of propagation. Therefore, the anterior pacing could easily capture the AP, because the angle of the excitation wavefront entered the AP was narrow. However, the posterior pacing could not capture AP because of the large angle resulting in an impedance mismatch (Fig. 4).

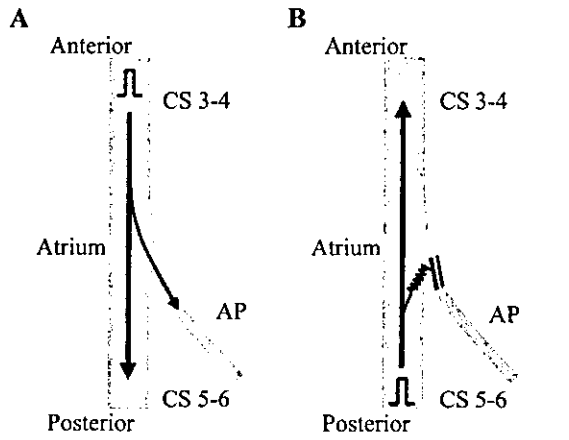

Fig. 4. The schema of the selective conduction block depending on the pacing site from coronary sinus (CS) electrodes. The excitation wavefront from anterior pacing with narrow angle toward the atrioventricular accessory pathway (AP) could easily conduct the AP (A). However, that from posterior pacing with wide angle toward the AP could not conduct the AP because of an impedance mismatch (B).

References

1. Spach MS, Miller V WT, Dolber JPC, Kootsey M, Sommer JR, Mosher Jr CE. The functional role of structural complexities in the propagation of depolarization in the atrium of the dog. *Circ Res* 1982;50:175–191.
2. Klein G, Yee R, Sharma AD. Concealed conduction in accessory atrioventricular pathways: An important determinant of the expression of arrhythmias in patients with Wolff-Parkinson-White syndrome. *Circulation* 1984;70:402–411.
3. Svinarich JT, Tai DY, Mickelson J, Keung EC, Sung RJ. Electrophysiologic determination of concealed conduction in anomalous atrioventricular bypass tracts. *J Am Coll Cardiol* 1985;5:898–903.
4. Przybylski J, Chiale PA, Sanchez RA, Pastori JD, Francos HG, Elizari MV, Rosenbaum MB. Supernormal conduction in the accessory pathway of patients with overt or concealed ventricular pre-excitation. *J Am Coll Cardiol* 1987;9:1269–1278.
5. Suzuki F, Harada T, Nawata H, Ohtomo K, Satoh T, Hirao K, Hiejima K. Retrograde supernormal conduction, gap phenomenon in concealed accessory atrioventricular pathway. *PACE*, 1992;15:1065–1079.
6. Gonzalez MD, Greenspon AJ, Kidwell GA. Linking in accessory pathways, Functional loss of antegrade preexcitation. *Circulation* 1991;83:1221–1231.
7. Suzuki F, Kawara T, Tanaka K, Harada T, Endoh T, Kanazawa Y, Okishige K, Hirao K, Hiejima K. Electrophysiological demonstration of antegrade concealed conduction in accessory atrioventricular pathways capable only of retrograde conduction. *PACE* 1989;12:591–603.
8. Fujiki A, Tani M, Mizumaki K, Yoshida S, Sasayama S. Rate-dependent accessory pathway conduction due to phase 3 and 4 block. *J Electrophysiol* 1992;25:25–31.
9. Ahn YK, Cho JG, Kim SH, Kim JW, Cho JH, Bae Y, Park JH, et al. A case of AV reentrant tachycardia due to a concealed accessory pathway with retrograde conduction manifested by isoproterenol. *Jpn Circ J* 1998;62:943–946.

10. Goldberger JJ, Pederson DN, Damle RS, Kim YH, Kadish AH. Antidromic tachycardia utilizing decremental, latent accessory atrioventricular fibers: Differentiation from adenosine-sensitive ventricular tachycardia. *J Am Coll Cardiol* 1994;24:732–738.

11. Otomo K, Gonzalez MD, Beckman KJ, et al. Reversing the direction of paced ventricular and atrial wavefronts reveals an oblique course in accessory AV pathways and improves localization for catheter ablation. *Circulation* 2001;104:550–556.

Ventricular Tachycardia Associated with Bidirectional Reentrant Circuit Around the Tricuspid Annulus in Arrhythmogenic Right Ventricular Dysplasia

TAKASHI NODA, KAZUHIRO SUYAMA, WATARU SHIMIZU, KAZUHIRO SATOMI, KIYOSHI OTOMO, EIICHIRO NAKAGAWA, TAKASHI KURITA, NAOHIKO AIHARA, and SHIRO KAMAKURA

From the Division of Cardiology, Department of Internal Medicine, National Cardiovascular Center, Suita, Japan

NODA, T., ET AL.: Ventricular Tachycardia Associated with Bidirectional Reentrant Circuit Around the Tricuspid Annulus in Arrhythmogenic Right Ventricular Dysplasia. *This case report describes two distinct morphological ventricular tachycardias (VTs) associated with bidirectional reentrant circuit around the tricuspid annulus in a 32-year-old patient with arrhythmogenic right ventricular dysplasia. Multiple radiofrequency linear ablation could abolish both VTs, and this patient has been clinically free from symptoms of VTs at 1-year follow-up. (PACE 2003; 26:2050–2051)*

ventricular tachycardia, ARVD, CARTO, ablation

Case Report

A 32-year-old man was referred to our hospital for recurrent episodes of ventricular tachycardias (VTs). He had first symptoms with palpitation and dizziness due to VTs at 30 years of age, and he was receiving 400 mg of amiodarone daily for the last 2 years as therapy for VTs. His standard 12-lead electrocardiogram, during sinus rhythm, showed incomplete right bundle branch block, epsilon waves, and inverted T waves in leads V_1 to V_4. Clinically, he had two distinct morphological VTs. The morphology of the first VT was left bundle branch block (LBBB) morphology with a superior QRS-axis deviation (Fig. 1A), while the second VT was LBBB morphology with an inferior QRS-axis deviation (Fig. 1B).

Further examination including cardiac angiograms, echocardiograms, magnetic resonance imaging, and radionuclide scintigraphy, indicated severe right ventricular (RV) dilatation and reduction of RV ejection fraction with no left ventricular involvement. He was diagnosed arrhythmogenic right ventricular dysplasia (ARVD) based on the criteria of international registry on ARVD,[1,2] and underwent an electrophysiological study with a three-dimensional electroanatomic mapping system (CARTO, Biosense Webster, Johnson & Johnson).[3,4] During sinus rhythm, the RV activation map by CARTO showed multiple delayed potentials in the posterolateral free wall of the RV near the tricuspid annulus (TA), and the RV bipolar voltage map indicated the diffuse area of extremely reduced voltage values in the posterolateral free wall of the RV. Programmed electrical stimulation (PES) was performed from the RV free wall, and VT was induced by double extrastimuli. This VT was the same morphology as the clinical first VT (LBBB morphology with a superior QRS-axis deviation) and was hemodynamically well tolerated (Fig. 1A). The RV activation map during the VT represented the circus movement around the TA. In the RV free wall (Fig. 1C), the wave front of activation proceeded in a craniocaudal direction, while it propagated in a caudocranial direction in the RV septal wall. Total activation time was nearly equal to the VT cycle length. Resetting could be demonstrated by a single extrastimulus during VT, delivered from the two different sites, not only lateral RV wall but also septal RV wall near the TA. In addition, the postpacing intervals (PPI) were equal to the VT cycle length at both sites. Resetting could be also shown by a single extrastimulus delivered from the anterior RV wall far from TA, but the PPI at this site was much longer than the VT cycle length. These observations indicated that the macroreentrant VT ran around the TA. Radiofrequency catheter linear ablation was performed during VT in the attempt to transect the anatomic isthmus between the scar area and the TA. The first linear lesion was created in the posterolateral free wall of the RV, but failed to interrupt the VT. Then, the second linear lesion was created in a more cranial site resulting in termination of the VT. However, as the clinical second VT (LBBB morphology with an inferior QRS-axis deviation), the next VT was induced by PES (Fig. 1B). This was also hemodynamically tolerated, thus the activation mapping of VT could be performed with CARTO. The circus

Address for reprints: Kazuhiro Suyama, M.D., Division of Cardiology, Department of Internal Medicine, National Cardiovascular Center, 5-7-1 Fujishiro-dai, Suita, Osaka, 565-8565 Japan. Fax: 81-6-6872-7486; e-mail: ksuyama@hsp.ncvc.go.jp

Received February 13, 2003; revised April 3, 2003; accepted May 3, 2003.

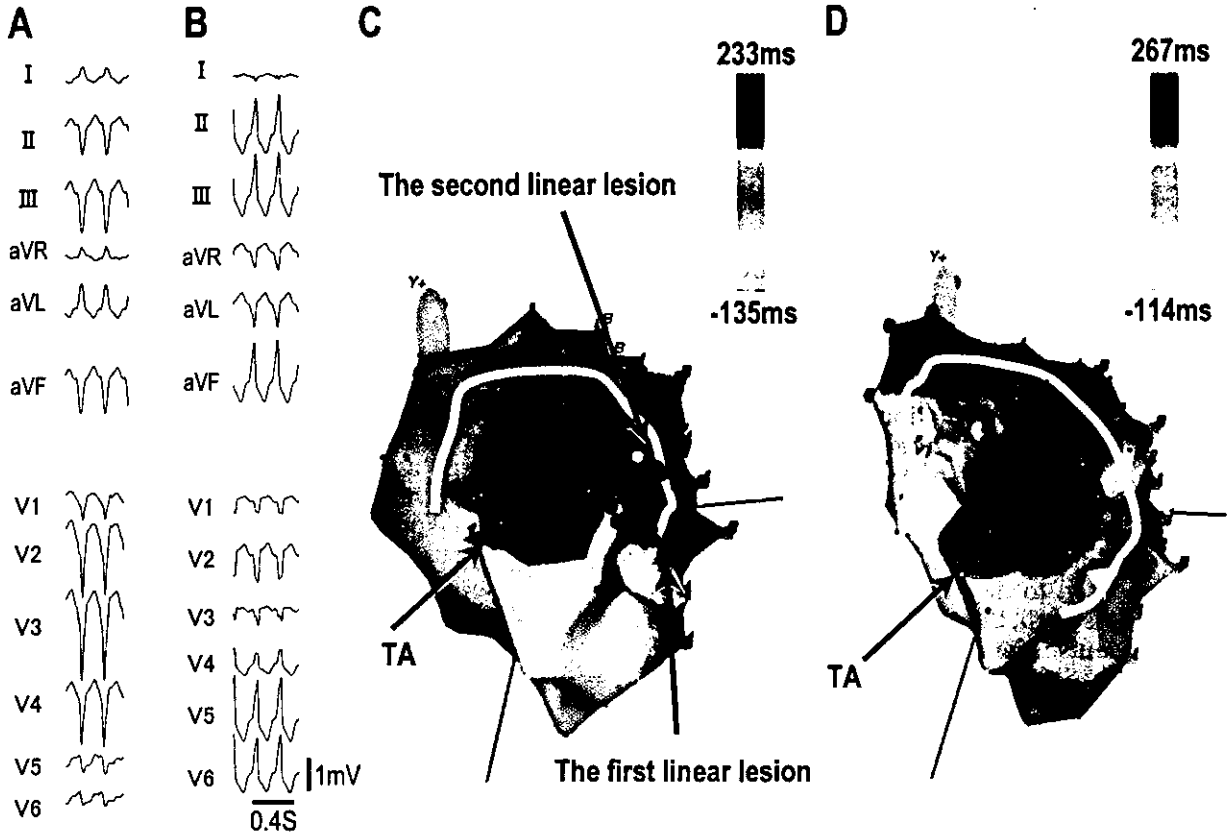

Figure 1. *(A) Twelve-lead ECG during the first ventricular tachycardia (VT). The morphology of the first VT was left bundle branch block (LBBB) morphology with a superior QRS-axis deviation. (B) Twelve-lead ECG during the second VT. The morphology of the second VT was LBBB morphology with a superior QRS-axis deviation. (C) The right posterior oblique view of the right ventricular (RV) activation map during the first VT by CARTO. The first VT revolved around the tricuspid annulus (TA). Note the wavefront of activation proceeded in a cranio-caudal direction in the RV free wall. Brown dots indicate radiofrequency applications. Red dot indicates the additional radiofrequency application to the gap of the second linear lesion. Gray areas represents scar (bipolar voltage amplitude ≤ 0.5 mV). (D) The right posterior oblique view of the RV activation map during the second VT by CARTO. The second VT also revolved around the TA. Note the wavefront of activation propagated in a reverse direction to the first VT in the RV free wall.*

movement around the TA was also shown but the wavefront of activation proceeded in the reverse direction (Fig. 1D). It was proved that the next VT was also resulting from a reentrant circuit around the TA. The additional radiofrequency application to the gap of the second linear lesion terminated the VT (red dot in Fig. 1C). After this procedure, PES could not induce either VT.

The patient has been clinically free from symptoms of VT at 1-year follow-up.

References

1. Corrado D, Fontaine G, Marcus FI, et al. Arrhythmogenic Right Ventricular Dysplasia/cardiomyopathy: Need for an international registry. Circulation 2000; 101:101e–106e.
2. Tada H, Shimizu W, Ohe T, et al. Usefulness of electron-beam computed tomography in arrhythmogenic right ventricular dysplasia. Relationship to electrophysiological abnormalities and left ventricular involvement. Circulation 1996; 94:437–444.
3. Boulos M, Lashevsky I, Reisner S, et al. Electroanatomic mapping of arrhythmogenic right ventricular dysplasia. J Am Coll Cardiol 2001; 38:2020–2027.
4. Ouyang F, Fotuhi P, Goya M, et al. Ventricular tachycardia around the tricuspid annulus in right ventricular dysplasia. Circulation 2001; 103:913–914.

A Simple and Accurate Method to Identify Early Ventricular Contraction Sites in Wolff-Parkinson-White Syndrome Using High Frame-Rate Tissue-Velocity Imaging

Yoko Miyasaka, MD, Satoshi Nakatani, MD, Kazuhiro Suyama, MD, Shiro Kamakura, MD, Mio Haiden, MD, Masakazu Yamagishi, MD, Masafumi Kitakaze, MD, Toshiji Iwasaka, MD, and Kunio Miyatake, MD

The high frame–rate tissue-velocity imaging method may be superior to the conventional M-mode method in accurately localizing accessory pathways without consuming large amounts of time. ©2003 by Excerpta Medica, Inc.

(Am J Cardiol 2003;92:617–620)

Recently developed high frame–rate tissue-velocity imaging (TVI) can be used to analyze regional myocardial velocities with excellent time resolution. By setting the region of interest on the 2-dimensional tissue Doppler image obtained, the regional myocardial velocity pattern is easily recognized. The purpose of this study was (1) to evaluate the feasibility of high frame–rate TVI for identifying early contraction sites in patients with Wolff-Parkinson-White (WPW) syndrome and (2) to compare the diagnostic capability of high frame–rate TVI and conventional M-mode method[1–5] using the successful ablation sites confirmed by invasive electrophysiologic study as the reference standard.

• • •

In this study, we prospectively enrolled 32 patients (22 men with a mean age 45 ± 18 years) with WPW syndrome who had been recommended to undergo electrophysiologic endocardial mapping and successful radiofrequency catheter ablation. An exclusion criterion for enrollment was a concealed bypass tract. No subjects had structural heart disease except for WPW syndrome, and all showed normal left ventricular function by conventional echocardiography. We also examined 21 control subjects (15 men with a mean age 58 ± 13 years) who had no evidence of structural heart disease and who had normal electrocardiographic, echocardiographic, and coronary angiographic results to define the normal myocardial velocity pattern obtained by high frame–rate TVI. Informed consent was obtained from each subject.

All patients were examined in the left lateral decubitus position with a commercially available ultrasound system (System FiVe; GE Vingmed, Horten, Norway) equipped with tissue Doppler imaging capabilities with a 3.5-MHz transducer. The frame rate could be kept up to 134 frames/s with the time resolution of approximately 7 ms. After a routine echocardiographic examination was performed, we obtained color tissue Doppler data the day before and within 3 days after the catheter ablation. The parasternal 2-dimensional short-axis view of the left ventricle at the mitral annular level was recorded with holding respiration at end-expiration. The bipolar limb lead electrocardiogram (I, II, or III) showing the clearest onset of the δ-wave was displayed on the ultrasound system monitor. Echocardiographic data were obtained by a single examiner (YM) who was blinded to 12-lead electrocardiographic data. Real-time images were stored in cine loop memory, thus permitting review.

High frame–rate TVI is a new technique that can be used to analyze the velocity of regional myocardium with excellent time resolution. By setting up to 8 regions of interest on the 2-dimensional tissue Doppler image obtained, regional myocardial velocity patterns can be easily mapped during a cardiac cycle. We regarded the site showing an abnormal presystolic contraction wave by the high frame–rate TVI as the early excitation site. We carefully analyzed the regional myocardial velocity patterns from various regions of interest on the 2-dimensional short-axis tissue Doppler image and searched the earliest contraction site during P-R interval on electrocardiogram using an analysis software (EchoPac, GE Vingmed)

Using the conventional M-mode echocardiographic method, we also carefully searched the earliest excitation site, which was characterized as the region showing an early inward endocardial motion before ventricular contraction. We compared the de-

TABLE 1 Identification of Early Excitation Sites in Wolff-Parkinson-White (WPW) Syndrome With the Use of High Frame–rate Tissue Velocity Imaging (TVI) and Conventional M-mode Echocardiography

	Number	High Frame–rate TVI (%)	Conventional M-mode (%)
Left-sided pathways	18	15 (83)	9 (50)
Right-sided pathways	14	9 (64)	4 (29)
Overall	32	24 (75)*	13 (41)

*$p < 0.05$ versus conventional M-mode echocardiography.

From the Cardiology Division of Medicine, National Cardiovascular Center, Suita; and the Cardiovascular Division, Department of Medicine II, Kansai Medical University, Moriguchi, Japan. This work was supported in part by a Research Grant for Cardiovascular Diseases from the Ministry of Health, Labor, and Welfare of Japan, Tokyo, Japan. Dr. Nakatani's address is: Cardiology Division of Medicine, National Cardiovascular Center, 5-7-1 Fujishiro-dai, Suita, Osaka 565-8565, Japan. E-mail: nakatas@hsp.ncvc.go.jp. Manuscript received March 5, 2003; revised manuscript received and accepted May 27, 2003.

0002-9149/03/$-see front matter
doi:10.1016/S0002-9149(03)00738-0

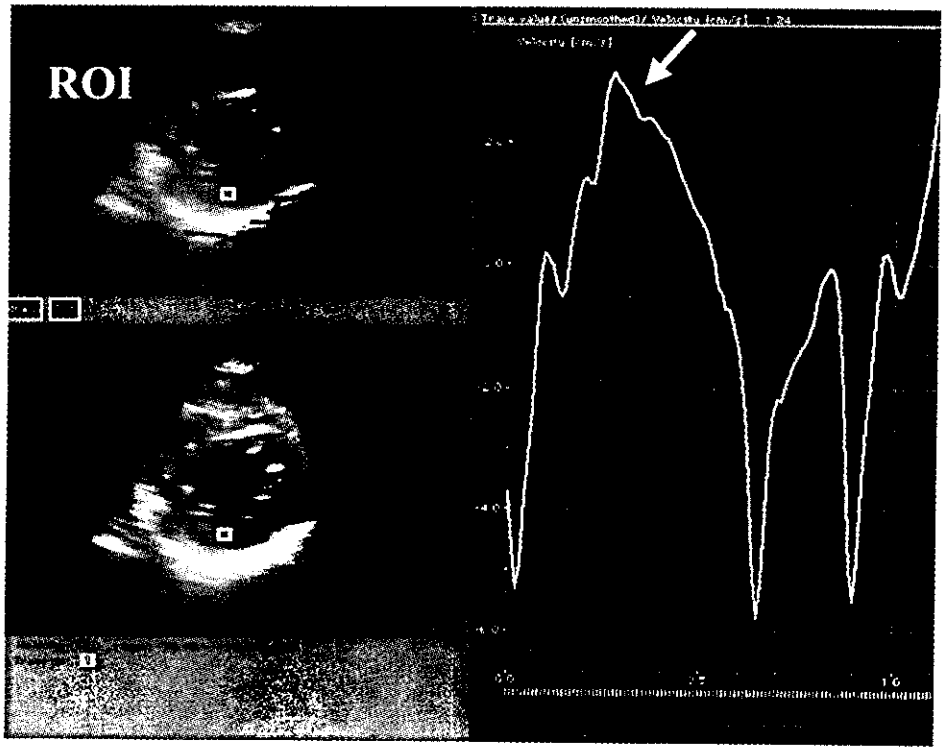

FIGURE 1. Example of a regional myocardial velocity pattern obtained by the high frame-rate TVI, displayed simultaneously with the electrocardiogram, in a normal control subject. Changes in regional myocardial velocity were recognized during 1 cardiac cycle. During systole, the monophasic velocity wave was observed *(white arrow)*. Note that there was no presystolic contraction wave just before the R wave. ROI = region of interest.

tection rate of an early excitation site using high frame-rate TVI with conventional M-mode methods employing the site determined by the invasive electrophysiologic study as the reference standard. The accessory pathway locations were classified into 10 regions on the atrioventricular groove as[6]: (1) left anterior, (2) left lateral, (3) left posterior, (4) left anteroseptal, (5) left posteroseptal, (6) right anterior, (7) right lateral, (8) right posterior, (9) right anteroseptal, and (10) right posteroseptal regions.

The indication of ablation was the existence of WPW syndrome, which caused potentially lethal arrhythmias or medically refractory frequent supraventricular tachycardias. The ablation procedure was performed according to standard techniques.[7] The location of an accessory pathway was defined by standard techniques, including (1) identifying the shortest atrioventricular times in sinus rhythm, (2) mapping the shortest ventriculoatrial conduction time during ventricular pacing or orthodromic reciprocating tachycardia, and (3) identifying an accessory pathway potential. Transcatheter radiofrequency ablation was performed according to standard methods. All subjects gave written informed consent for the ablation procedure.

All data were expressed as mean ± SD. Comparisons of the detection rate of accessory pathway locations by high frame-rate TVI with conventional M-mode echocardiographic method were analyzed using the chi-square test. A value of $p < 0.05$ was considered statistically significant.

The detection rate of determination of early excitation sites using conventional M-mode echocardiographic method compared with the successful ablation sites is shown in Table 1. The early excitation sites were unrecognized in 15 (left anterior in 1, left lateral in 4, right anterior in 1, right lateral in 5, and right posteroseptal in 4) and misdiagnosed in 4 (left anterior in 1 and left lateral in 3) subjects.

In control subjects, no presystolic contraction wave was observed anywhere on the left ventricular short-axis image (Figure 1). In contrast, when the region of interest was set on the early excitation site in patients with WPW syndrome, an abnormal presystolic contraction wave was recognized (Figures 2 and 3). This abnormal early contraction wave was represented at the time of the δ-wave or just before the R-wave on the electrocardiogram; it formed a biphasic wave together with the systolic contraction wave. The presystolic contraction wave was not recognized on areas other than the early excitation site in subjects with WPW syndrome (Figure 2).

The feasibility of determining early excitation sites using the high frame-rate TVI technique compared with the successful ablation sites as confirmed by invasive electrophysiologic study is shown in Figure 4. The early excitation sites were unrecognized in 5 (left lateral in 1, right lateral in 2, and right posteroseptal in 2) and misdiagnosed in 3 (left lateral in 2, and right lateral in 1) subjects. Early contraction sites determined by high frame-rate TVI agreed well with the successful ablation sites. After successful catheter ablation, presystolic contraction waves were not detected more often by high frame-rate TVI in all patients.

Using the high frame-rate TVI technique, the detection rate of early excitation sites was improved

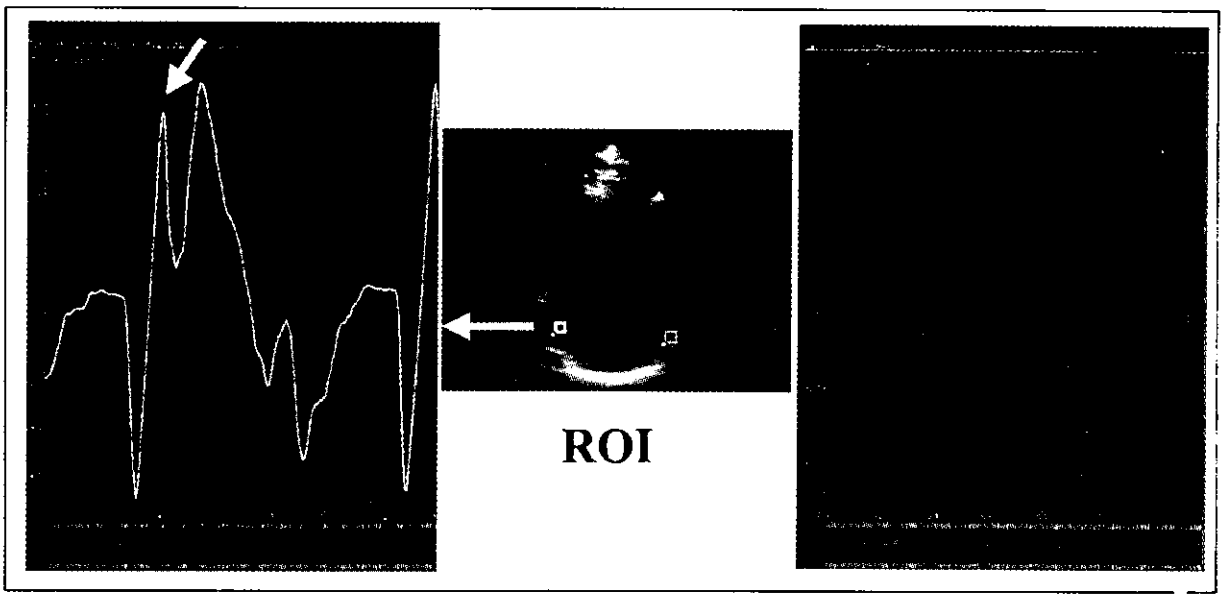

FIGURE 2. Example of a regional myocardial velocity pattern occurring during a cardiac cycle taken from a subject having WPW syndrome with a left posterior accessory pathway. On the early excitation site, an abnormal presystolic contraction wave *(white arrow)* and systolic contraction wave formed a biphasic wave *(left panel)*. This abnormal early contraction wave was represented at the time of the δ-wave on the electrocardiogram. On sites other than the early excitation site, abnormal presystolic contraction wave was not recognized (right panel). Abbreviation as in Figure 1.

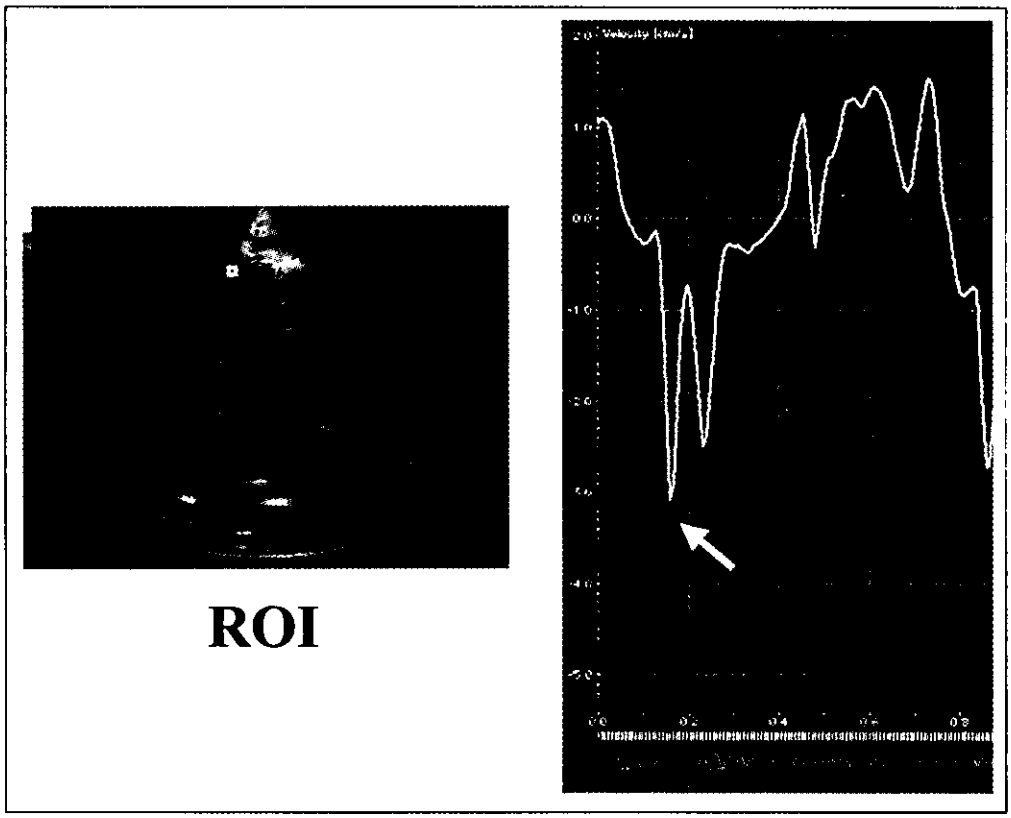

FIGURE 3. Examples of a regional myocardial velocity pattern occurring during a cardiac cycle taken from a subject having WPW syndrome with a right anterior accessory pathway. On the early excitation site, an abnormal presystolic contraction wave *(white arrow)* was represented at the time of the δ-wave on the electrocardiogram. Abbreviation as in Figure 1.

compared with the use of conventional M-mode echocardiography (Table 1). Overall prediction of the accessory pathway localization using high frame–rate TVI was significantly superior to that using the conventional M-mode echocardiographic method.

• • •

In this study, we evaluated the feasibility of the recently developed high frame–rate TVI for identifying early contraction sites in 32 patients with WPW syndrome before and after successful radiofrequency catheter ablation. Our results showed that the high frame–rate TVI technique was superior to the conventional M-mode method in identifying early excitation sites, especially in patients with right-sided accessory pathways.

High frame–rate TVI can be used to analyze the

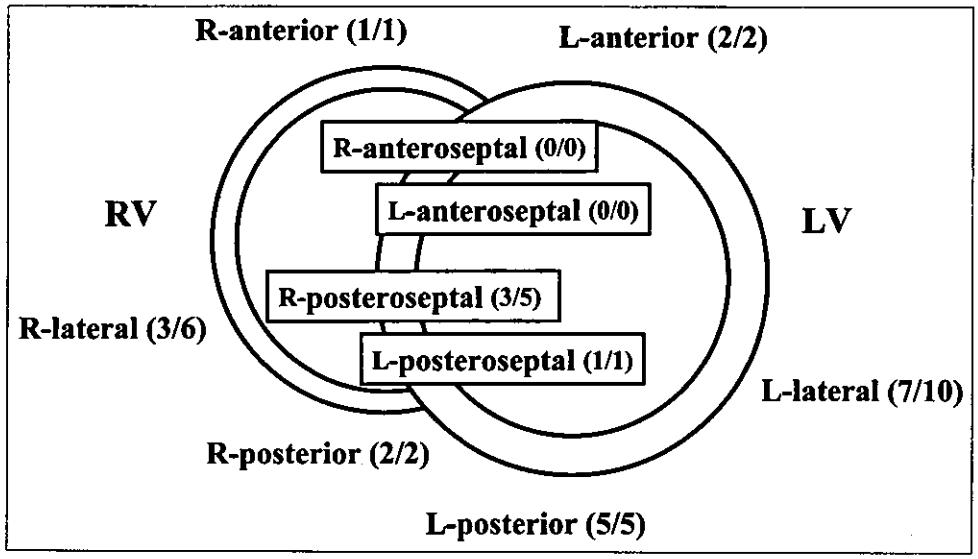

FIGURE 4. The feasibility of determining early excitation sites, with regard to location using high frame-rate TVI. Numbers in parentheses represent the incidence of identification compared with the sites of accessory pathways confirmed by the invasive catheter-based electrophysiologic study. L = left; LV = left ventricle; R = right; RV = right ventricle.

velocity of moving structures with excellent time resolution of approximately 7 ms. By simply setting the region of interest on the 2-dimensional image obtained, pinpoint and regional myocardial velocity pattern are easily recognized during a cardiac cycle. High frame-rate TVI has several advantages compared with previous echocardiographic methods,[1-5] including conventional tissue Doppler methods.[8-13] Using this method, the accessory pathway location can be clearly and easily recognized by visual estimation as an abnormal presystolic contraction wave. Moreover, even if the quality of the 2-dimensional echocardiographic image was suboptimal, we could enhance the sensitivity for detection of early contraction site because pulsed Doppler information is less affected by tissue attenuation than M-mode and 2-dimensional imaging. This should allow the recognition of early excitation site even in patients with poor acoustic windows.

1. DeMaria AN, Vera Z, Neumann A, Mason DT. Alterations in ventricular contraction pattern in the Wolff-Parkinson-White syndrome: detection by echocardiography. *Circulation* 1976;53:249–257.
2. Chandra NS, Kerber RE, Brown DD, Funk DC. Echocardiography in Wolff-Parkinson-White syndrome. *Circulation* 1976;53:943–946.
3. Francis GS, Theroux P, O'Rourke RA, Hagan AD, Johnson AD. An echocardiographic study of interventricular septal motion in the Wolff-Parkinson-White syndrome. *Circulation* 1976;54:174–178.
4. Hishida H, Sotobata I, Koike Y, Okumura M, Mizuno Y. Echocardiographic patterns of ventricular contraction in the Wolff-Parkinson-White syndrome. *Circulation* 1976;54:567–570.
5. Ticzon AR, Damato AN, Caracta AR, Russo G, Foster JR, Lau SH. Interventricular septal motion during preexcitation and normal contraction in Wolff-Parkinson-White syndrome: echocardiographic and electrophysiologic correlation. *Am J Cardiol* 1976;37:840–847.
6. Windle JR, Armstrong WF, Feigenbaum H, Miles WM, Prystowsky EN. Determination of the earliest site of ventricular activation in Wolff-Parkinson-White syndrome: application of digital continuous loop two-dimensional echocardiography. *J Am Coll Cardiol* 1986;7:1286–1294.
7. Lesh MD, van Hare GF, Schamp DJ, Chien W, Lee MA, Griffin JC, Langberg JJ, Cohen TJ, Lurie KG, Scheinman MM. Curative percutaneous catheter ablation using radiofrequency energy for accessory pathways in all locations: results in 100 consecutive patients. *J Am Coll Cardiol* 1992;19:1303–1309.
8. Nakayama K, Miyatake K, Uematsu M, Tanaka N, Kamakura S, Nakatani S, Yamazaki N, Yamagishi M. Application of tissue Doppler imaging technique in evaluating early ventricular contraction associated with accessory atrioventricular pathways in Wolff-Parkinson-White syndrome. *Am Heart J* 1998;135:99–106.
9. Nagai H, Takata S, Sakagani S, Furusho H, Takamura M, Kobayashi K. Two-dimensional guided M-mode color tissue Doppler echocardiography in artificial preexcitation models. *J Am Soc Echocardiogr* 1999;12:582–589.
10. Nagai H, Takata S, Sakagami S, Furusho H, Takamura M, Yuasa T, Kobayashi K. Detection of the earliest ventricular contraction site in patients with Wolff-Parkinson-White syndrome using two-dimensional guided M-mode tissue Doppler echocardiography. *Cardiology* 1999;92:189–195.
11. Tuchnitz A, Schmitt C, von Bibra H, Schneider MAE, Plewan A, Schomig A. Noninvasive localization of accessory pathways in patients with Wolff-Parkinson-White syndrome with the use of myocardial Doppler imaging. *J Am Soc Echocardiogr* 1999;12:32–40.
12. Yin LX, Li CM, Fu QG, Lo Y, Huang QH, Cai L, Zheng ZX. Ventricular excitation maps using tissue Doppler acceleration imaging: potential clinical application. *J Am Coll Cardiol* 1999;33:782–787.
13. Eder V, Marchal C, Tranquart F, Sirinelli A, Pottier JM, Cosnay P. Localization of the ventricular preexcitation site in Wolff-Parkinson-White syndrome with Doppler tissue imaging. *J Am Soc Echocardiogr* 2000;13:995–1001.